

RESEARCH

Open Access



# TAM-derived exosomal miR-589-3p accelerates ovarian cancer progression through BCL2L13

Jianqing Wang<sup>1†</sup>, Yan Zhu<sup>1†</sup>, Yang He<sup>1</sup> and Weiwei Shao<sup>2,3\*</sup>

## Abstract

**Background** Tumor-associated macrophages (TAM) are critical elements of intercellular communication in tumor microenvironment (TME), and exosomes are key mediators between tumor cells and the TME. According to previous reports, miRNAs exert a pivotal role in ovarian cancer (OC) development. The purpose of this work was to explore the function of TAM-derived exosomal miR-589-3p in OC development and elucidate the underlying molecular mechanisms.

**Methods** First, peripheral blood mononuclear cells (PBMC) were treated with IL-4 and IL-13 to polarize them into M2-type macrophages. Exosomes were separated from M2-type macrophages, and the physical properties of exosomes were evaluated using transmission electron microscopy (TEM) and nanoparticle tracking analysis (NTA). Next, quantitative reverse-transcriptase polymerase chain reaction (qRT-PCR) was applied to examine the expression of relevant genes. Subsequently, Targetscan and miRDB were utilized to predict miR-589-3p target genes, and then the interaction between miR-589-3p and BCL2L13 was verified by dual luciferase assay and RNA Binding Protein Immunoprecipitation (RIP) assay. Finally, Cell Counting Kit-8 (CCK-8) and flow cytometry experiments were employed to explore the changes in the proliferative and apoptotic abilities of OC cells.

**Results** In this research, we demonstrated that TAM-derived exosomes facilitated OC cell proliferation and suppressed OC cell apoptosis. Then, qRT-PCR results indicated that miR-589-3p were markedly elevated after co-culture of TAM-derived exosomes with OC cells. In addition, we discovered that miR-589-3p was bound to BCL-2-like protein 13 (BCL2L13), which was confirmed through luciferase assay and RIP assay. Furthermore, functional analysis displayed that TAM-derived exosomes treated with miR-589-3p inhibitor attenuated the promotion of OC cell progression by exosomes.

**Conclusion** TAM-derived exosomal miR-589-3p enhanced OC progression through BCL2L13, which offers a novel for OC therapy.

**Keywords** TAM, Exosome, miR-589-3p, BCL2L13, OC

<sup>†</sup>Jianqing Wang and Yan Zhu contributed equally to this work.

\*Correspondence:

Weiwei Shao  
maggie\_sww@sina.com

<sup>1</sup>Department of Gynecology and Obstetrics, Yancheng First People's Hospital, Yancheng Clinical College of Xuzhou Medical University, Yancheng, Jiangsu 224002, China

<sup>2</sup>Department of Pathology, Yancheng First People's Hospital, Yancheng Clinical College of Xuzhou Medical University, Yancheng, Jiangsu 224002, China

<sup>3</sup>Department of Pathology, Yancheng Clinical College of Xuzhou Medical University, Yancheng First People's Hospital, No. 166, Yulong West Road, Yancheng, Jiangsu 224002, China



© The Author(s) 2025. **Open Access** This article is licensed under a Creative Commons Attribution-NonCommercial-NoDerivatives 4.0 International License, which permits any non-commercial use, sharing, distribution and reproduction in any medium or format, as long as you give appropriate credit to the original author(s) and the source, provide a link to the Creative Commons licence, and indicate if you modified the licensed material. You do not have permission under this licence to share adapted material derived from this article or parts of it. The images or other third party material in this article are included in the article's Creative Commons licence, unless indicated otherwise in a credit line to the material. If material is not included in the article's Creative Commons licence and your intended use is not permitted by statutory regulation or exceeds the permitted use, you will need to obtain permission directly from the copyright holder. To view a copy of this licence, visit <http://creativecommons.org/licenses/by-nc-nd/4.0/>.

## Introduction

Ovarian cancer (OC) is a type of gynecologic malignancy and the eighth most common cause of cancer deaths in women worldwide. In 2020, there were more than 310,000 new cases and about 200,000 deaths, which is a serious threat to women's lives and health [1]. Clinically, the onset of OC is relatively insidious, and the absence of early diagnostic markers coupled with the metastatic nature of the tumor results in a poor prognosis for patients [2]. Currently, the standard therapy for OC is surgery together with chemotherapy [3]. In spite of the fact that the prognosis of patients with OC has markedly progressed with surgery and chemotherapy, the survival rate of OC patients remains poor [4], which is due to the fact that most of the OC patients are already in advanced stages when they are detected and some of the OC patients have developed chemoresistance after therapy [5]. Hence, seeking potential biomarkers is clinically important for early screening and improving the prognosis of OC patients.

For the past several years, the critical function of tumor microenvironment (TME) in tumorigenesis and development has been recognized. Tumor-associated macrophages (TAMs) are one of the most abundant immune cells in the tumor microenvironment and present at all stages of tumor progression [6]. TAMs have a range of biological functions, such as induction of tumor progression, angiogenesis, metastasis, and treatment resistance [7]. Studies have shown that TAMs secrete large quantities of EGF to activate EGFR in surrounding tumor cells, promoting OC cell growth, migration, adhesion, and spheroid formation [8]. In addition, TAM facilitates migration of high-grade plasmacytoid OC cells by secreting TGFBI and TNC [9]. These previous findings revealed that TAM acts a vital role in OC progression. Nevertheless, the mechanisms underlying the role of TAMs in OC have not been fully characterized.

There is growing proof that TAMs regulated cancer advancement by secreting exosomes [10]. Exosomes are extracellular vesicles that mediate intercellular communication by transferring proteins, noncoding RNA (ncRNA), etc., from TAMs to tumor cells [11]. For example, TAM-secreted exosomes transferred hsa\_circ\_0001610 into endometrial cancer cells to reduce the radiosensitivity of endometrial cancer [12]. Another study demonstrated that TAM-derived exosomal miR-95 accelerated prostate cancer cell growth and invasion by directly binding to JunB [13]. The role of TAMs in promoting tumorigenesis is obvious, yet how TAM-derived exosomes affect OC progression has not been elucidated.

MiRNAs are the most abundant ncRNAs in exosomes. Exosome-borne miRNAs have the ability to be ingested by nearby or distant cells, thereafter they suppress target mRNAs in recipient cells to facilitate oncogenic signaling

[14]. Aberrant expression of exosomal miRNAs affects interaction between cancer cells and TME [15]. Specifically, in gastric cancer, exosomal transfer of TAM-derived miR-21 confers cisplatin tolerance to gastric cancer cells [16]. TAM-derived exosomes confer gemcitabine tolerance to pancreatic adenocarcinoma by transferring miR-365 [17]. miR-589-3p is a multifunctional miRNA involved in a wide range of biological activities. miR-589-3p has been demonstrated to affect tumor proliferation or metastasis in a range of tumors types, such as glioblastoma, breast cancer, and gastric cancer [18]. Nevertheless, whether miR-589-3p from TAM-derived exosomes are involved in OC progression still needs to be further investigated.

The aim of our study was to investigate the impact of TAM-derived exosomal miR-589-3p on OC cell progression. In this study, we first constructed M2 macrophages activated by IL-4 and IL-13, successfully isolated exosomes from M2-type macrophages, and confirmed that TAM-derived exosomes facilitated OC cell progression. Subsequently, miR-589-3p was disclosed to be clearly heightened after co-culture of M2 macrophage-derived exosomes and OC cells using qRT-PCR. miR-589-3p transferred from TAM to OC cells through exosomes and promote OC progression. Further investigation demonstrated that miR-589-3p affected OC progression by targeting BCL-2-like protein 13 (BCL2L13). Our findings may offer a perspective therapy target for OC patients.

## Materials and methods

### Cell culture and processing

OC cells (SKOV3, CAO3) were purchased from Type Culture Preservation Center of the Chinese Academy of Sciences Cell Bank. Cells were cultivated in DMEM (Gibco) containing 10% fetal bovine serum (FBS), 100 U/mL penicillin and 100 µg/ml streptomycin at 37 °C, 5% CO<sub>2</sub>.

Human peripheral blood mononuclear cells (PBMC) were purchased from Shanghai Huzhen Biotechnology (Shanghai, China). Monocytes were isolated from PBMCs by negative selection using magnetic beads (MiltenyiBiotec), and then the isolated cells were cultured in RPMI 1640 supplemented with 10% exosome-free FBS (Gibco) and 25 ng/ml M-CSF for 7 days to induce the maturation of monocytes to macrophages. The medium was changed every 3 days to discard contaminated non-adherent cells and harvest adherent cells. Subsequently, 20 ng/ml IL-4 coupled with 20 ng/ml IL-13 (PeproTech, USA) was added to culture the cells for 48 h to acquire M2 polarized macrophages.

### Co-culture system

Macrophages and OC cells were co-cultured using the transwell co-culture system. For co-culture experiments,

macrophages were cultured in the upper chamber of the transwell (Corning) with a pore size of 0.4  $\mu\text{m}$ , and OC cells were cultivated in the lower chamber of the transwell. To inhibit exosome release from macrophages, macrophages were treated with the exosome inhibitor GW4869 (5  $\mu\text{M}$ ).

#### Isolation of macrophage exosomes

Cell cultures were centrifuged at 1,000 g 5 min, followed by centrifugation at 15,000 g 15 min at 4  $^{\circ}\text{C}$ , and then filtered through a 0.22  $\mu\text{m}$  filter membrane to exclude dead cells and cellular debris. After that, the supernatant was centrifuged at 110,000 g 70 min. The precipitate was gathered and resuspended in PBS.

#### Transmission electron microscopy (TEM)

Under transmission electron microscopy, 10  $\mu\text{l}$  of exosome suspension was dropped on a 200-mesh copper grid and incubated for 1 min. The samples were washed with double-distilled water and incubated with 2% phosphotungstic acid solution for 1 min. After air-drying, the samples were observed under a TEM-1400plus at 80 kV.

#### Nanotracking analysis (NTA)

The exosome samples were diluted to 1 ml with ultrapure water and placed into the sample tank of the nanoparticle size analyzer Zetasizer Nano for automatic sample uptake, during which the ratio of dilution was adjusted according to the situation. Finally, the nanoparticles were captured and data analyzed using the NTA analysis software that comes with the system.

#### Cell transfection

miR-589-3p mimic, NC mimic, miR-589-3p inhibitor, NC inhibitor, si-BCL2L13#1 and si-BCL2L13#2, si-NC were synthesized through RiboBio (Guangzhou, China). Cells were inoculated in 6-well plates ( $5 \times 10^6$ ) and transfected after their growth was stabilized. Cells were transfected with Lipofectamine 3000 (Invitrogen). The medium was changed after 6 h of incubation, and the cells were collected following 72 h.

#### Quantitative reverse-transcriptase polymerase chain reaction (qRT-PCR)

Total RNA was obtained from the cells through TRIzol reagent (Takara, China). Nanodrop 2000 system (Nanodrop Technologies, USA) was applied to assess RNA quality and concentration. cDNA was synthesized via reverse transcription using the reverse transcription kit (Takara, China). qRT-PCR reactions were applied using SYBR Premix ExTaq (Takara, China) and ABI Prism 7900HT (Applied Biosystems, USA). Relative level was calculated using the  $2^{-\Delta\Delta\text{Ct}}$  method. The primer sequences used in the qRT-PCR were as follows:

miR-589-3p F 5'-AACAAATGCCGGTTCACAGA-3'.  
R 5'-TGTCGTGGAGTCGGCAATTG-3'.  
BCL2L13 F 5'-AGGACTATTCGGCAGAGTACAT-3'.  
R 5'-TGATTCCAGGGTATTCCTCCTC-3'.  
GAPDH F 5'-GGCAAATTCATGGCACCGT-3'.  
R 5'-GCATCGCCCCACTTGATTTT-3'.  
U6: F 5'-TGCGGTGGGTGTCATCAA-3'.  
R 5'-AACGCTTCACGAATTTGGT-3'.

#### Western blot (WB)

Total protein was extracted by lysing cell samples on ice using lysis buffer. Next, quantification was performed using an enhanced BCA kit (Beyotime, China). 20  $\mu\text{g}$  protein samples were separated by 10% SDS-PAGE. Following their separation, the proteins were moved to a polyvinylidene difluoride membrane. After blocking with 5% BSA, the membrane was incubated with primary antibodies at 4  $^{\circ}\text{C}$  overnight. After primary antibody incubation, HRP-labeled secondary antibody was added to continue the incubation. Finally, the protein blotting signals were visualized by an enhanced chemiluminescence detection kit (Beyotime, China).

#### Cell counting Kit-8 (CCK-8) experiment

Cells were inoculated into 96-well plates ( $3 \times 10^3$ ). After 24 h of incubation, 10  $\mu\text{L}$  of CCK-8 solution was added. Then, the cells were incubated at 37  $^{\circ}\text{C}$  for 2 h. Absorbance at 450 nm was determined by a microplate reader to assess cell viability at different 0 h, 24 h, 48 h and 72 h, respectively.

To assess the effect of TAMs-derived exosomes on OC cell proliferation, TAMs-derived exosomes were co-cultured with SKOV3 or CAO3, and changes in cell viability were detected at different time. To assess the effect of exosomes miR-589-3p derived from TAMs on cell proliferation, exosomes were extracted after transfection of miR-589-3p inhibitor in TAMs, and SKOV3 or CAO3 cells were treated with exosomes to detect changes in cell viability at different time.

#### Apoptosis test

Apoptosis was detected by the FITC Annexin V Apoptosis Detection Kit (BD Pharmagen, USA). After giving the cells two thorough rinses with cold PBS, they were resuspended in 100  $\mu\text{l}$  of 1 $\times$  binding buffer. Following this, 5  $\mu\text{l}$  of FITC Annexin V and 5  $\mu\text{l}$  of propidium iodide (PI) staining were added, and they were left to incubate for 15 min in the absence of light. After that, 400  $\mu\text{l}$  of 1 $\times$  binding buffer was added and then analyzed by flow cytometry.

#### RNA binding protein immunoprecipitation (RIP) assay

RIP RNA-binding protein immunoprecipitation kit (Millipore, USA) was utilized to perform RIP assay. Cells were

lysed on ice-cold lysate, and then centrifuged at 1500 rpm 15 min. Protein extracts were incubated with anti-AGO2 and control IgG (Millipore, USA) in reverse rotation overnight. Afterwards, approximately 30  $\mu$ L of protein beads were introduced and the cells were suspended. Following this, the cells were incubated at 4 °C for four hours. The isolated RNA was analyzed by qRT-PCR.

#### Luciferase experiment

Based on the bioinformatics software TargetScan and miRDB, we predicted the potential target genes of miRNAs. We constructed BCL2L13 wild-type (BCL2L13-wt) and mutant (BCL2L13-mut) reporter vectors and inserted them into the pGL3 vector (GenePharma, China). The BCL2L13-wt and BCL2L13-mut plasmids were co-transfected with miR-589-3p mimic and its NC mimic into 293T cells through Lipofectamine 3000. 48 h later, a dual luciferase reporter kit (Promega) was used to measure the luciferase activity.

#### Statistical analysis

Data were expressed as mean  $\pm$  standard deviation and plotted utilizing GraphPad Prism 8.0 software. Analyses between the two groups were employed by Student's t-test. Analysis between multiple groups was employed by one-way analysis of variance (ANOVA). Differences were considered statistically significant at  $P < 0.05$ .

## Results

#### Extraction and characterization of TAM-derived exosomes

To assess the role of exosomes in OC, we treated PBMC with IL-4 and IL-13 to polarize them into M2 macrophages in vitro. Exosomes were subsequently isolated from M2 macrophages utilizing ultracentrifugation. TEM, NTA, and WB assay was employed to characterize the cell supernatant exosomes. TEM observed that the extracted exosomes displayed a vesicular structure with a double membrane (Fig. 1A). NTA displayed that the diameter of the double-layered ring vesicles ranged from 100 to 200 nm (Fig. 1B). WB results discovered that the exosome marker proteins (CD63, CD81, TSG101 and HSC70) were remarkably enhanced in exosomes (Fig. 1C). The above experimental results confirmed that we successfully extracted exosomes from M2 macrophages.

#### TAM-derived exosomes facilitate proliferation and repress apoptosis of OC cells

To evaluate the functional biological effects of TAM-derived exosomes on OC cells in vitro, we co-cultured TAM-secreted exosomes with SKOV3 and CAOV3 to investigate the influence of TAM-derived exosomes on SKOV3 and CAOV3 cells. The results of CCK-8 revealed that a marked raise in the proliferative capacity

of SKOV3 and CAOV3 after co-culture. Subsequently, M2 macrophages were treated with the exosome inhibitor GW to inhibit exosome release. It was found that this was significantly attenuated by GW-treated macrophages (Fig. 2A). Next, the influence of TAM-secreted exosomes on apoptosis of SKOV3 and CAOV3 was examined using flow cytometry. The outcomes indicated that TAM-derived exosomes dramatically reduced SKOV3 and CAOV3 cell apoptosis compared to control, which was reversed by the addition of GW (Fig. 2B, C). In addition, we performed dose-dependent apoptosis experiments using the apoptosis inducer-carbonyl cyanide 3-chlorophenylhydrazone (CCCP) and investigated the effects of co-treatment with EXO and CCCP apoptosis inducers on apoptosis in SKOV3 and CAOV3 cells. The results revealed a dose-dependent increase in the apoptotic capacity of the cells after CCCP treatment. Moreover, the apoptotic ability of cells in the EXO + CCCP-treated group was significantly decreased compared with CCCP treatment, suggesting that exosomes have certain anti-apoptotic effects (Fig. S1A-B). These observations meant that M2 macrophage-derived exosomes enhanced OC cell proliferation and restrained apoptosis.

#### TAM-derived exosomal miR-589-3p enhances OC cell proliferation and depresses apoptosis

There is evidence that miRNAs engaged in intercellular communication are often contained in exosomes, which allow them to carry out their biological activities in recipient cells. To probe the mechanism of TAM-derived exosomes in OC development, we disclosed that miR-589-3p was remarkably elevated in TAM-derived exosomes co-cultured with SKOV3 and CAOV3 cells via qRT-PCR assay (Fig. 3A). To ascertain whether exosomes promote OC progression through miR-589-3p, we transfected miR-589-3p inhibitor or NC inhibitor in TAM. qRT-PCR results disclosed that the level of exosomal miR-589-3p was suppressed after transfection of miR-589-3p inhibitor in M2 macrophages (Fig. 3B). Subsequently, the levels of miR-589-3p in SKOV3 and CAOV3 cells were detected after treatment with exosomes transfected with miR-589-3p inhibitor. miR-589-3p was found to significantly decrease (Fig. 3C). Afterwards, changes in cell viability and apoptosis were measured using CCK-8 assay kit and flow cytometry. As a matter of fact, TAM derived exosomes transfected with miR-589-3p inhibitor reversed the promoting effect of exosomes on cell proliferation and the inhibitory effect on cell apoptosis (Fig. 3D-F). In summary, TAM-derived exosomal miR-589-3p contributed malignant advancement of OC cells.

#### BCL2L13 is a downstream target of miR-589-3p

To explore the mechanism by which miR-589-3p affects OC progression, the target genes of miR-589-3p were

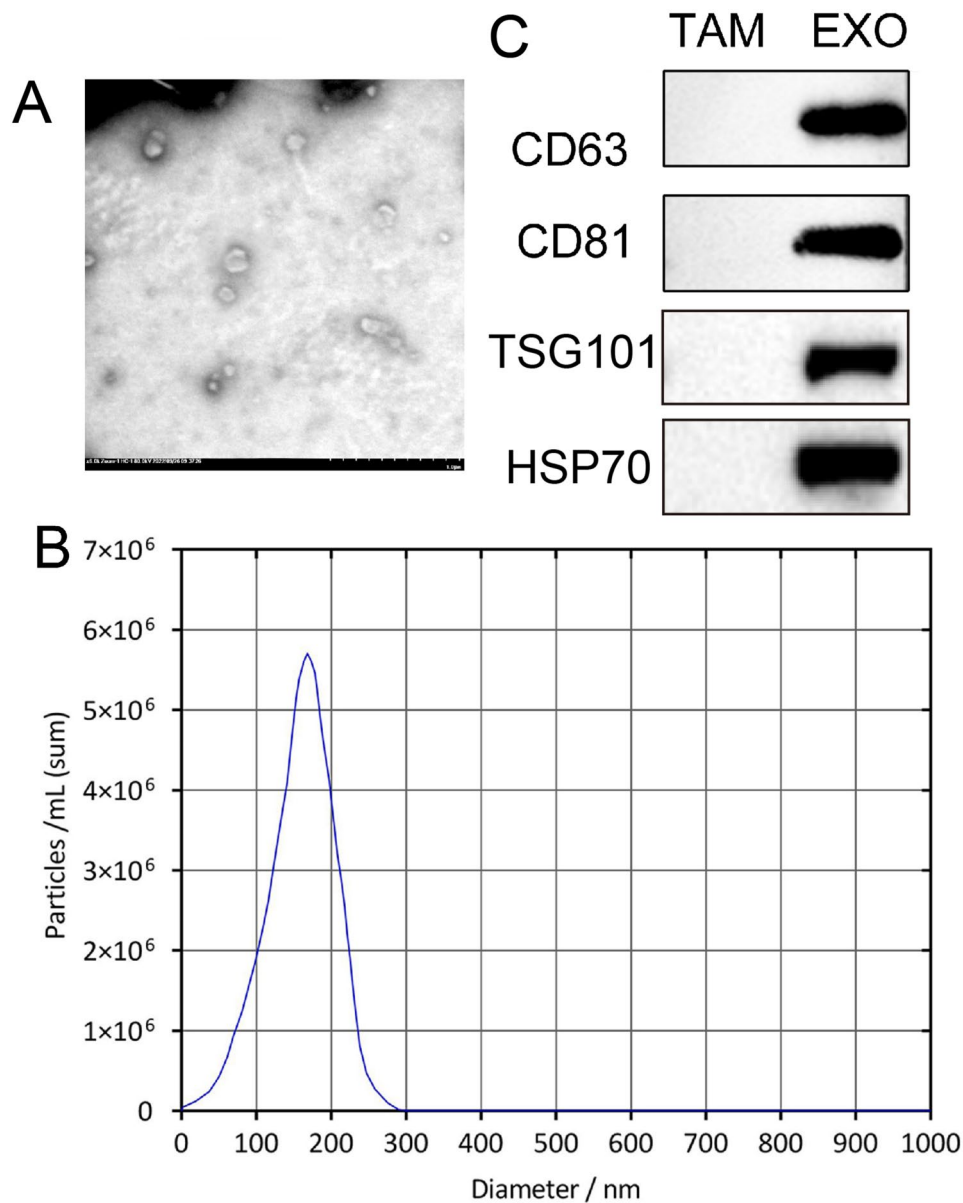


**Fig. 1** Extraction and characterization of TAM-derived exosomes. **(A)** Transmission electron microscopy was used to observe the morphology of exosomes isolated from M2-type macrophages; **(B)** Zetasizer Nano particle size analyzer was applied to determine the M2-type macrophage-derived exosome particle size; **(C)** Western blot was utilized to detect the content of exosome markers (CD63, CD81, TSG101, and HSC70)

searched by miRDB and Targetscan, and apoptosis-related genes were selected to take the intersection. The results revealed that there were five apoptosis-related genes (Fig. 4A). Subsequently, qRT-PCR was performed to determine the impact of miR-589-3p knockdown on the above genes, and the findings confirmed that BCL2L13 was elevated in SKOV3 and CAOV3 cells the most after knocking down miR-589-3p, so we guessed that BCL2L13 was the target gene of miR-589-3p (Fig. 4B). Moreover, whether BCL2L13 has a binding site to miR-589-3p was predicted by Targetscan website. The outcome indicated that miR-589-3p bound to

the 3' UTR region of BCL2L13 (Fig. 4C). Next, luciferase and RIP experiments were used to verify the binding relationship between miR-589-3p and BCL2L13. The outcomes of luciferase assay displayed that miR-589-3p mimic remarkably weakened the luciferase activity of WT-BCL2L13, whereas the luciferase activity of MUT-BCL2L13 was not significantly changed (Fig. 4D). The results of RIP assay disclosed that BCL2L13 was notably enriched in anti-Ago2 contrasted to anti-IgG. The above findings confirmed a binding association between miR-589-3p and BCL2L13 (Fig. 4E). Furthermore, qRT-PCR and WB results indicated that the level of BCL2L13 was

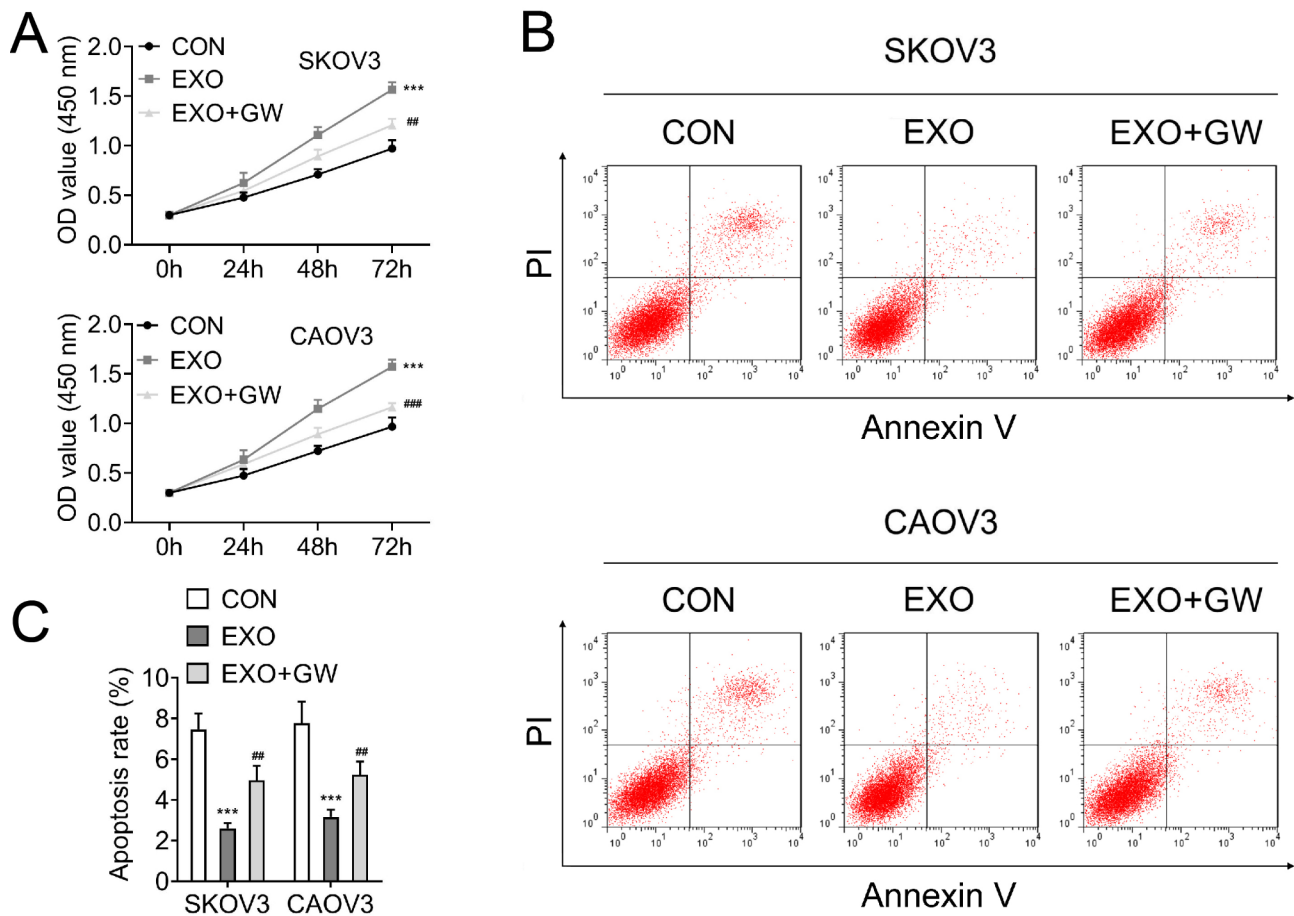


**Fig. 2** TAM-derived exosomes facilitate proliferation and repress apoptosis of OC cells. **(A)** CCK-8 assay was used to detect the changes in SKOV3 and CAOV3 cell viability at 0 h, 24 h, 48 h, and 72 h after treatment with exosomes and/or the exosome inhibitor GW (5  $\mu$ M); **(B)** Flow cytometry was utilized to determine the effects of exosomes and/or exosome inhibitor GW (5  $\mu$ M) treatment on SKOV3 and CAOV3 cell apoptosis; **(C)** The SKOV3 and CAOV3 cells quantification of apoptosis rate

clearly reduced after co-culture of TAM-derived exosomes with SKOV3 and CAOV3 cells (Fig. 4F). These outcomes manifested that BCL2L13 was a downstream target of miR-589-3p.

#### BCL2L13 silencing reverses the effect of miR-589-3p knockdown on cell progression

Next, BCL2L13 was knockdown in SKOV3 and CAOV3 cells, and changes in BCL2L13 expression were detected by qRT-PCR. The transfection efficiency was examined through qRT-PCR and WB, and the findings displayed that the BCL2L13 was markedly diminished after knockdown of BCL2L13, indicating that the transfection was successful. Among them, the knockdown efficiency of si-BCL2L13#2 was higher, so si-BCL2L13#2 was used for subsequent experiments (Fig. 5A). Next, the cell growth was observed via CCK-8 test, and we identified that BCL2L13 silencing reversed the suppressive action of miR-589-3p knockdown on cell growth (Fig. 5B). In addition, flow cytometry findings disclosed

an increased percentage of apoptosis after transfection with miR-589-3p inhibitor, however, this phenomenon was rescued by co-transfection of miR-589-3p inhibitor with si-BCL2L13 (Fig. 5C, D). Furthermore, the apoptotic capacity of cells in the inhibitor + CCCP-treated group was significantly elevated compared to the CCCP treatment (Fig S2A). The above outcomes demonstrated that BCL2L13 knockdown abolished the impact of miR-589-3p silencing on cell progression.

#### Discussion

OC is one of the more lethal of female malignant tumors and has a poor prognosis [19]. An in-depth comprehension of the specific mechanisms of OC development could vastly benefit the outcome of OC patients. In this research, we identified the mechanism by which TAM-derived exosomes accelerated OC progression. Our data elucidated that the TAM-derived exosomal miR-589-3p facilitated OC advancement by suppressing BCL2L13 expression.

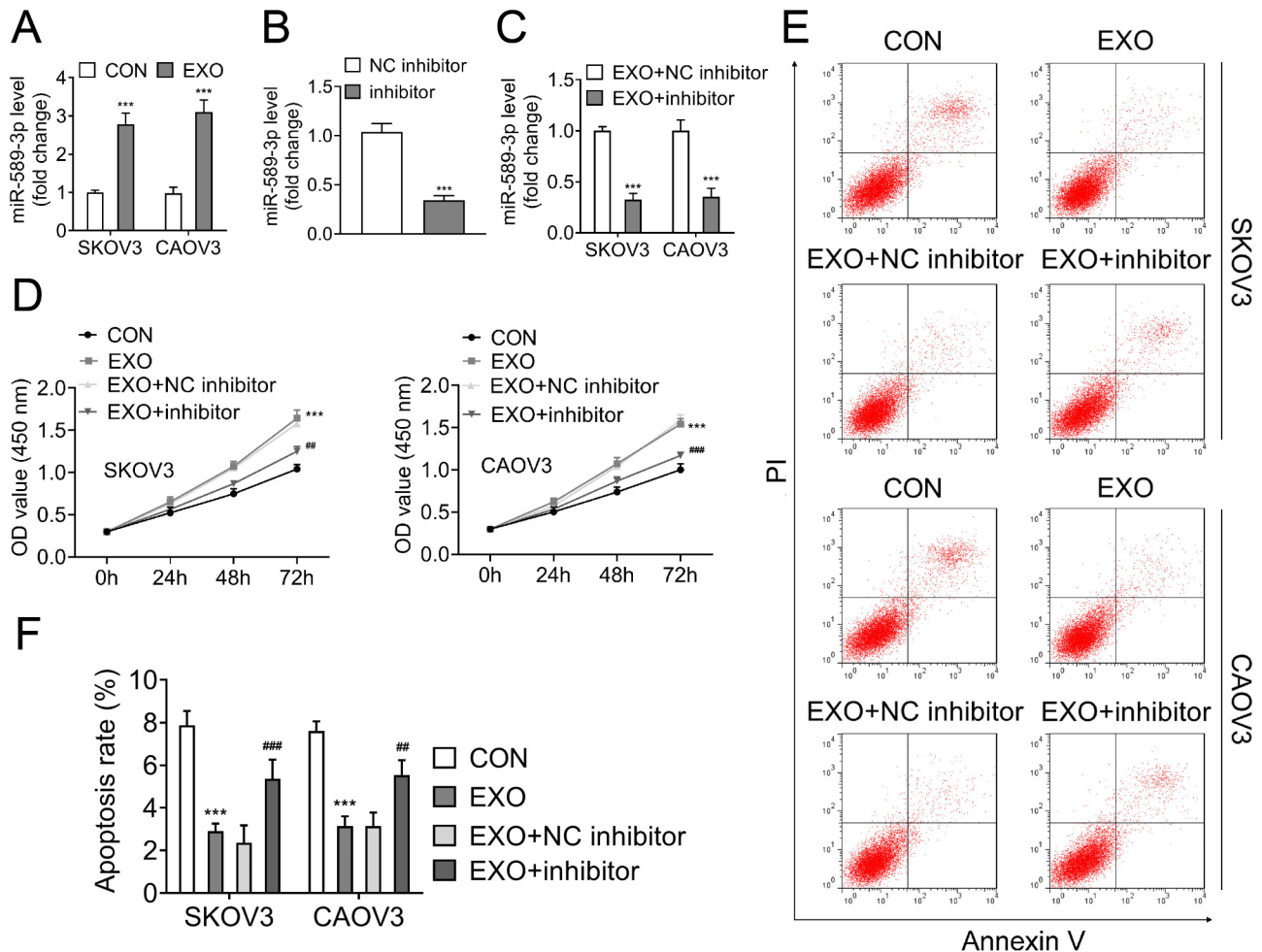


**Fig. 3** TAM-derived exosomal miR-589-3p enhances OC cell proliferation and depresses apoptosis. Exosomes were extracted after transfection of miR-589-3p inhibitor or NC inhibitor in TAM and then SKOV3 and CAOV3 cells were treated with exosomes. **(A)** qRT-PCR was performed to detect the expression of miR-589-3p after co-culture of TAM-derived exosomes with SKOV3 and CAOV3 cells; **(B)** qRT-PCR was performed to detect the level of exosomal miR-589-3p after transfection with miR-589-3p inhibitor in M2 macrophages; **(C)** qRT-PCR was applied to detect the level of miR-589-3p in cells after treatment of SKOV3 and CAOV3 cells with exosomes transfected with miR-589-3p inhibitor; **(D)** CCK-8 experiment was performed to measure the changes in SKOV3 and CAOV3 cell viability at 0 h, 24 h, 48 h and 72 h after treatment of SKOV3 and CAOV3 cells with exosomes transfected with miR-589-3p inhibitor; **(E)** Flow cytometry was performed to detect the changes in apoptotic capacity after treatment of SKOV3 and CAOV3 cells with exosomes transfected with miR-589-3p inhibitor; **(F)** The quantification of apoptosis rate in SKOV3 and CAOV3 cells

TME has a major function in tumor progression and metastasis. TAM is one of the major groups of TME, with two main phenotypes, M1 and M2. M1 macrophages are pro-inflammatory, whereas M2 macrophages are able to promote tumorigenesis and progression, and it has been demonstrated that M2-type macrophages are closely associated with tumor neovascularization, tumor growth and metastasis, and tumor drug resistance [20]. In this research, IL-4 and IL-13 were used to induce PBMC differentiation into M2-type macrophages to mimic TAM. It was pointed out that in addition to cytokine-mediated tumor-immune cells interactions, exosome also serve a crucial function in TME [21]. Exosomes are bilayer lipid extracellular vesicles. It has been shown to mediate material transfer and information exchange between cells [22].

Previous studies have demonstrated that circ\_0020256 in exosomes secreted by TAM stimulated the growth and metastasis of cholangiocarcinoma cells, whereas this stimulation was mediated through the circ\_0020256/miR-432-5p/E2F3 [23]. In addition, miR-223-3p in TAM-derived exosomes was delivered to 4T1 cells to enhance lung metastasis of 4T1 cells via Cbx5 [24]. A recent study indicated that the exosomal LINC01232 generated by TAM induced immune escape from glioma through reducing surface MHC-I level [25]. At this research, we successfully isolated exosomes from TAM cells and subsequently found TAM-secreted exosomes facilitated OC cell growth and inhibited apoptosis, which was reversed by treatment with the exosome inhibitor GW, implying

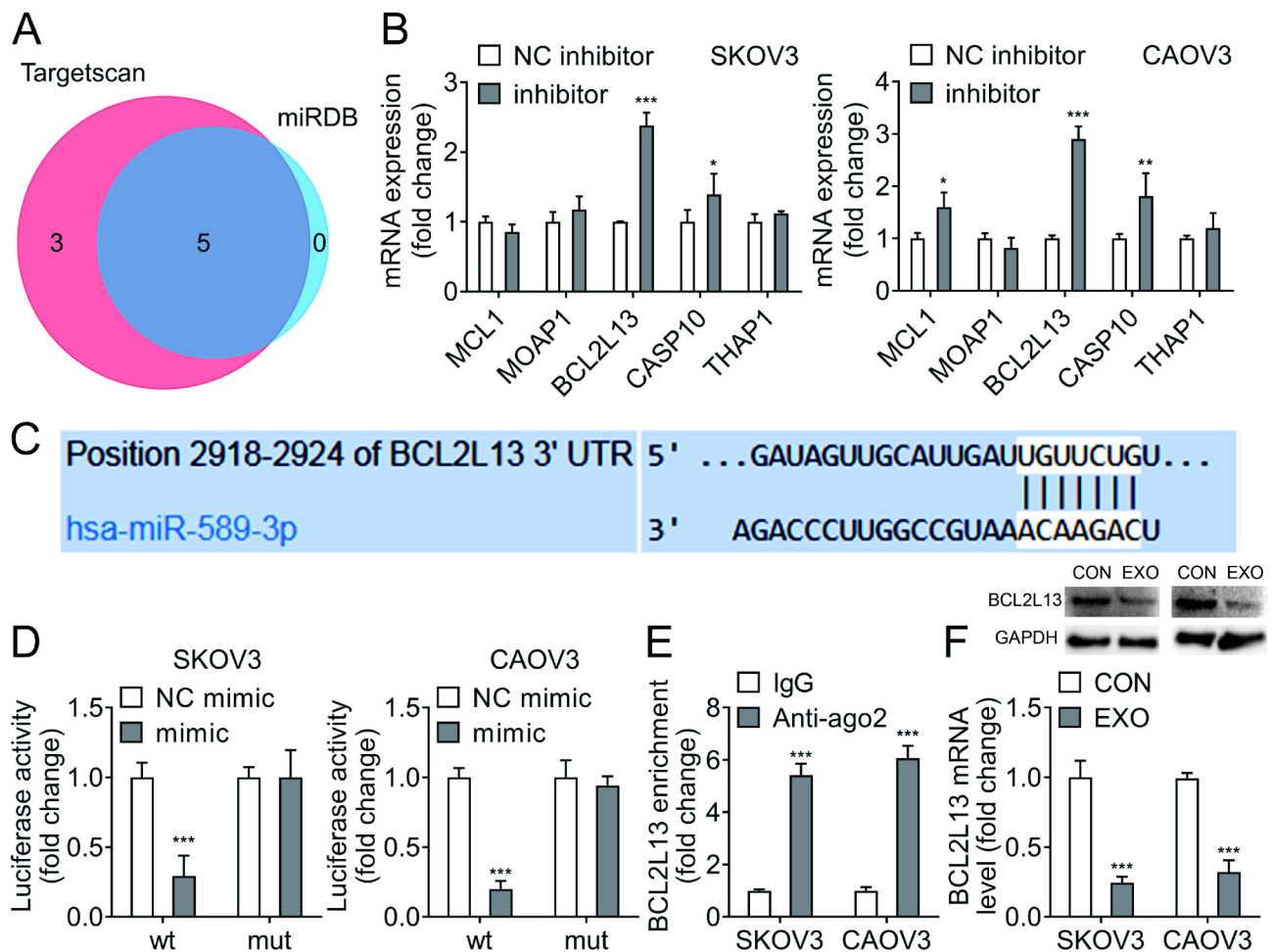


**Fig. 4** BCL2L13 is a downstream target of miR-589-3p. **(A)** Targetscan and miRDB were used to predict the miR-589-3p target genes, and apoptosis-related genes were selected to take the intersection; **(B)** qRT-PCR was performed to detect the effect of miR-589-3p knockdown on the expression of the above genes; **(C)** Targetscan website was applied to predict the binding site between miR-589-3p and BCL2L13; **(D)** Luciferase reporter assay was used to verify the binding relationship between miR-589-3p and BCL2L13; **(E)** Ago2-RIP-PCR was used to verify the binding relationship between miR-589-3p and BCL2L13; **(F)** qRT-PCR and western blot was used to detect the level of BCL2L13 in TAM-derived exosomes co-cultured with SKOV3 and CAOV3 cells

that exosomes may be the main mediator of crosstalk between OC cells and TAMs.

Numerous studies have shown that dysregulated miRNAs are important regulators of various tumorigenesis [26]. miRNAs are non-protein-coding RNA transcripts of 21–25 nucleotides in length, which can effectively regulate gene expression after gene transcription [27]. In addition, miRNAs have been found to be enriched in exosomes as well. For instance, the tumor-secreted exosomal miR-934 facilitated colorectal cancer liver metastasis via inducing macrophage M2 polarization [28]. The exosomal miR-205 secreted by OC cells accelerated cell metastasis by activating angiogenesis [29]. Many studies reveal the role of miR-589-3p in cancer. For example, as a sponge of lncRNA TINCR, miR-589-3p suppressed the Akt pathway via IGF1R, which repressed the proliferation and metastasis of breast cancer cells and stimulated apoptosis [30]. Moreover, ADAR2 regulated glioblastoma

cell invasion and migration through miR-589-3p [31]. In this project, we found miR-589-3p was raised after co-culture of TAM-secreted exosomes and SKOV3 and CAOV3 cells via qRT-PCR. Exosomes were extracted after transfection of TAM with miR-589-3p inhibitor, and then SKOV3 and CAOV3 cells were treated with exosomes to study the influence of exosomal miR-589-3p on cell growth and apoptosis. The outcomes manifested that miR-589-3p inhibitor alleviated the promotion of cell proliferation and inhibition of apoptosis by exosomes. These findings demonstrated the important function of exosomal miR-589-3p secreted by TAM in OC proliferation and the mechanism by which miR-589-3p facilitated tumor progression in a unique exosome-mediated manner.

To further disclose the specific mechanism of miR-589-3p regulating OC proliferation, we identified that the target of miR-589-3p was BCL2L13 by bioinformatic



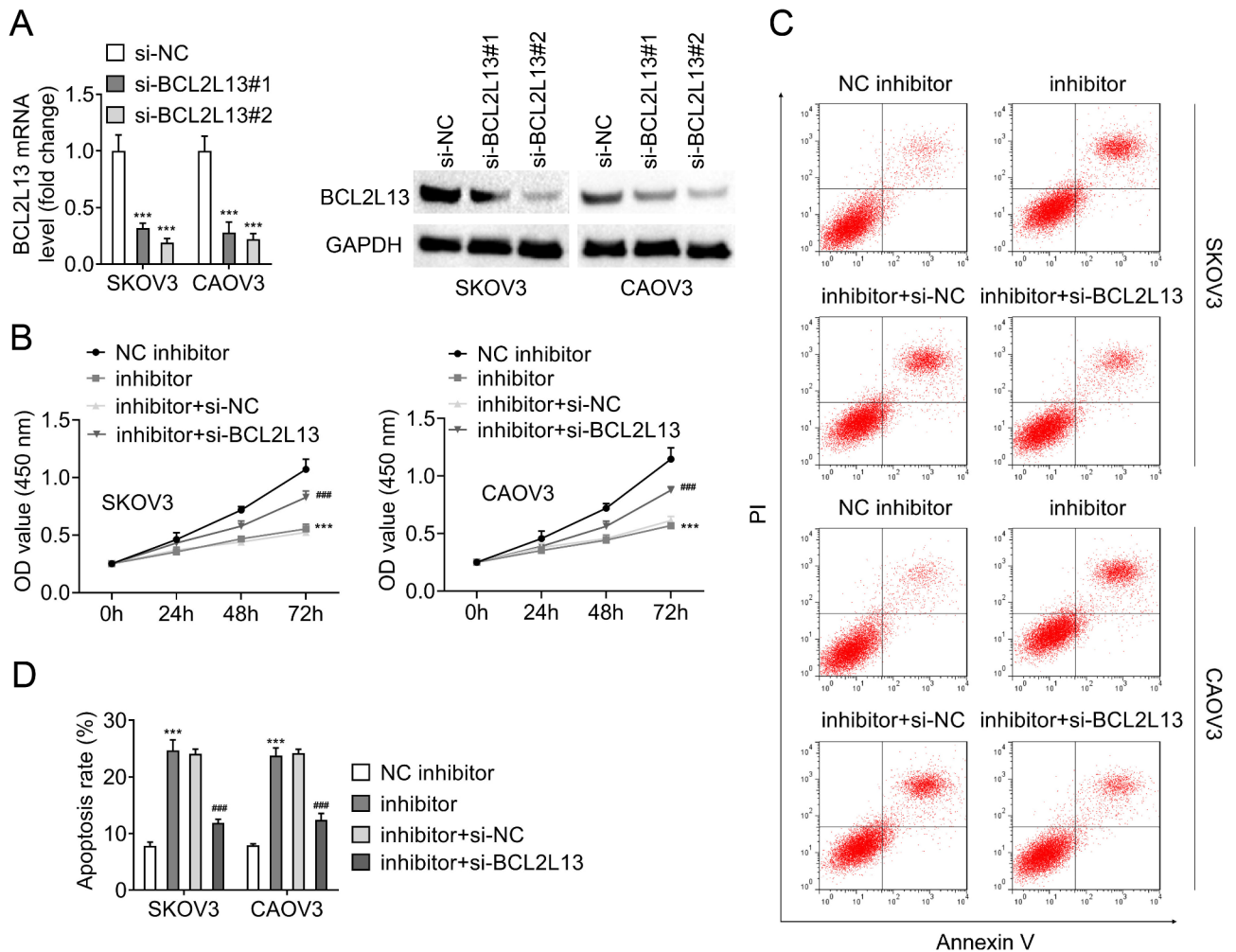


**Fig. 5** BCL2L13 silencing reverses the effect of knockdown of miR-589-3p on cell progression. **(A)** qRT-PCR and western blot was applied to detect the changes of BCL2L13 expression after transfection with si-NC, si-BCL2L13#1, si-BCL2L13#2 in SKOV3 and CAOV3 cell lines; **(B)** CCK-8 was used to detect the changes of SKOV3 and CAOV3 cell viability at 0 h, 24 h, 48 h, and 72 h after knockdown of miR-589-3p and/or knockdown of BCL2L13 treatment in SKOV3 and CAOV3 cells; **(C)** Flow cytometry was performed to detect the effect of knockdown of miR-589-3p and/or knockdown BCL2L13 treatment on SKOV3 and CAOV3 cell apoptosis; **(D)** The quantification of apoptosis rate in SKOV3 and CAOV3 cells

analysis. BCL-2-like protein 13 (BCL2L13) is also called BCL-rambo. BCL2L13 is part of the BCL2 family of proteins, with an intact BCL2 homology 1–4 structural domain, and its protein product exhibits the ability to mediate apoptosis in a variety of cell lines [32]. BCL2L13 has been discovered to be engaged in the advancement of several illnesses. The circRNA BBS9 inhibitor was reported to inhibit cigarette smoke extract-induced apoptosis of human lung microvascular endothelial cells via miRNA-103a-3p/BCL2L13, suggesting a crucial action in chronic obstructive pulmonary disease [33]. In renal cell carcinoma, BCL2L13 expression is downregulated and correlated with poor patients prognosis [34]. Wang et al. disclosed that BCL2L13 stimulated mitosis in glioblastoma through DNMT1L, and that the regulatory and biological functions of BCL2L13 make it a target for the treatment of glioblastoma [35]. According to

our results, the expression of BCL2L13 in exosomes co-culture with OC cells was clearly reduced, suggesting that BCL2L13 was associated with the progression of OC. Further analysis displayed that knockdown of BCL2L13 returned the inhibitory influence of miR-589-3p inhibitor on cell growth and the promotion of apoptosis. It revealed that miR-589-3p accelerated cell proliferation through BCL2L13, thereby facilitating the progression of OC.

In summary, TAM-derived exosomes run a critical role in OC development, and the TAM-derived exosomal miR-589-3p facilitated OC cell proliferation and weakened apoptosis through BCL2L13. This study provides new insights into the association between OC cells and TAM and highlights the possibility of exosomal miR-589-3p as a new target for OC treatment.

## Supplementary Information

The online version contains supplementary material available at <https://doi.org/10.1186/s13048-025-01618-1>.

Supplementary Material 1

Supplementary Material 2

### Acknowledgements

Not applicable.

### Author contributions

J.W. and Y.Z. designed the study, performed the experiments, and drafted the manuscript. Y.H. collected data, processed statistical data, and performed the experiments. W.S. designed, supervised the study, and revised the manuscript. All authors read and approved the final version of the manuscript.

### Funding

Not applicable.

### Data availability

No datasets were generated or analysed during the current study.

### Declarations

#### Ethics approval and consent to participate

Not applicable.

#### Clinical trial number

Not applicable.

#### Competing interests

The authors declare no competing interests.

Received: 9 July 2024 / Accepted: 5 February 2025

Published online: 21 February 2025

## References

1. Sung H, Ferlay J, Siegel RL, Laversanne M, Soerjomataram I, Jemal A, et al. Global Cancer statistics 2020: GLOBOCAN estimates of incidence and Mortality Worldwide for 36 cancers in 185 countries. *CA Cancer J Clin*. 2021;71(3):209–49.
2. Kuroki L, Guntupalli SR. Treatment of epithelial ovarian cancer. *BMJ*. 2020;371:m3773.
3. Wang Z, Meng F, Zhong Z. Emerging targeted drug delivery strategies toward ovarian cancer. *Adv Drug Deliv Rev*. 2021;178:113969.
4. Baert T, Ferrero A, Sehoul J, O'Donnell DM, González-Martín A, Joly F, et al. The systemic treatment of recurrent ovarian cancer revisited. *Ann Oncol*. 2021;32(6):710–25.
5. Chiappa M, Guffanti F, Bertoni F, Colombo I, Damia G. Overcoming PARPi resistance: preclinical and clinical evidence in ovarian cancer. *Drug Resist Updat*. 2021;55:100744.
6. Pan Y, Yu Y, Wang X, Zhang T. Tumor-Associated macrophages in Tumor Immunity. *Front Immunol*. 2020;11:583084.
7. Garimella R, Eskew J, Bhamidi P, Vielhauer G, Hong Y, Anderson HC, et al. Biological characterization of preclinical bioluminescent osteosarcoma Orthotopic Mouse (BOOM) model: a multi-modality approach. *J Bone Oncol*. 2013;2(1):11–21.
8. Yin M, Li X, Tan S, Zhou HJ, Ji W, Bellone S, et al. Tumor-associated macrophages drive spheroid formation during early transcoelomic metastasis of ovarian cancer. *J Clin Invest*. 2016;126(11):4157–73.
9. Steitz AM, Steffes A, Finkernagel F, Unger A, Sommerfeld L, Jansen JM, et al. Tumor-associated macrophages promote ovarian cancer cell migration by secreting transforming growth factor beta induced (TGFB1) and tenascin C. *Cell Death Dis*. 2020;11(4):249.
10. Xu Z, Chen Y, Ma L, Chen Y, Liu J, Guo Y, et al. Role of exosomal non-coding RNAs from tumor cells and tumor-associated macrophages in the tumor microenvironment. *Mol Ther*. 2022;30(10):3133–54.
11. Wortzel I, Dror S, Kenific CM, Lyden D. Exosome-mediated metastasis: communication from a Distance. *Dev Cell*. 2019;49(3):347–60.
12. Gu X, Shi Y, Dong M, Jiang L, Yang J, Liu Z. Exosomal transfer of tumor-associated macrophage-derived hsa\_circ\_0001610 reduces radiosensitivity in endometrial cancer. *Cell Death Dis*. 2021;12(9):818.
13. Guan H, Peng R, Fang F, Mao L, Chen Z, Yang S, et al. Tumor-associated macrophages promote prostate cancer progression via exosome-mediated miR-95 transfer. *J Cell Physiol*. 2020;235(12):9729–42.
14. Qin X, Guo H, Wang X, Zhu X, Yan M, Wang X, et al. Exosomal miR-196a derived from cancer-associated fibroblasts confers cisplatin resistance in head and neck cancer through targeting CDKN1B and ING5. *Genome Biol*. 2019;20(1):12.
15. Yang F, Ning Z, Ma L, Liu W, Shao C, Shu Y, et al. Exosomal miRNAs and miRNA dysregulation in cancer-associated fibroblasts. *Mol Cancer*. 2017;16(1):148.
16. Zheng P, Chen L, Yuan X, Luo Q, Liu Y, Xie G, et al. Exosomal transfer of tumor-associated macrophage-derived miR-21 confers cisplatin resistance in gastric cancer cells. *J Exp Clin Cancer Res*. 2017;36(1):53.
17. Binenbaum Y, Fridman E, Yaari Z, Milman N, Schroeder A, Ben David G, et al. Transfer of miRNA in macrophage-derived Exosomes induces Drug Resistance in pancreatic adenocarcinoma. *Cancer Res*. 2018;78(18):5287–99.
18. Shi F, He R, Zhu J, Lu T, Zhong L. Mir-589-3p promoted osteogenic differentiation of periodontal ligament stem cells through targeting ATF1. *J Orthop Surg Res*. 2022;17(1):221.
19. Li H, Luo F, Jiang X, Zhang W, Xiang T, Pan Q et al. CircITGB6 promotes ovarian cancer cisplatin resistance by resetting tumor-associated macrophage polarization toward the M2 phenotype. *J ImmunoTher Cancer* 2022;10(3).
20. Chanmee T, Ontong P, Konno K, Itano N. Tumor-associated macrophages as major players in the tumor microenvironment. *Cancers (Basel)*. 2014;6(3):1670–90.
21. Adamo A, Brandi J, Caligola S, Delfino P, Bazzoni R, Carusone R, et al. Extracellular vesicles mediate mesenchymal stromal cell-dependent regulation of B Cell PI3K-AKT signaling pathway and actin cytoskeleton. *Front Immunol*. 2019;10:446.
22. El-Saghir J, Nassar F, Tawil N, El-Sabban M. ATL-derived exosomes modulate mesenchymal stem cells: potential role in leukemia progression. *Retrovirology*. 2016;13(1):73.
23. Chen S, Chen Z, Li Z, Li S, Wen Z, Cao L, et al. Tumor-associated macrophages promote cholangiocarcinoma progression via exosomal Circ\_0020256. *Cell Death Dis*. 2022;13(1):94.
24. Wang Z, Zhang C, Guo J, Wang W, Si Q, Chen C, et al. Exosomal miRNA-223-3p derived from tumor associated macrophages promotes pulmonary metastasis of breast cancer 4T1 cells. *Transl Oncol*. 2023;35:101715.
25. Li J, Wang K, Yang C, Zhu K, Jiang C, Wang M, et al. Tumor-Associated Macrophage-Derived Exosomal LINC01232 induces the Immune escape in Glioma by decreasing surface MHC-I expression. *Adv Sci (Weinh)*. 2023;10(17):e2207067.
26. Zhang H, Yang K, Ren T, Huang Y, Tang X, Guo W. Mir-16-5p inhibits chordoma cell proliferation, invasion and metastasis by targeting Smad3. *Cell Death Dis*. 2018;9(6):680.
27. Farshbaf A, Mohtasham N, Zare R, Mohajertehran F, Rezaee SA. Potential therapeutic approaches of microRNAs for COVID-19: challenges and opportunities. *J Oral Biol Craniofac Res*. 2021;11(2):132–7.
28. Zhao S, Mi Y, Guan B, Zheng B, Wei P, Gu Y, et al. Tumor-derived exosomal miR-934 induces macrophage M2 polarization to promote liver metastasis of colorectal cancer. *J Hematol Oncol*. 2020;13(1):156.
29. He L, Zhu W, Chen Q, Yuan Y, Wang Y, Wang J, et al. Ovarian cancer cell-secreted exosomal miR-205 promotes metastasis by inducing angiogenesis. *Theranostics*. 2019;9(26):8206–20.
30. Guo F, Zhu X, Zhao Q, Huang Q. miR-589-3p sponged by the lncRNA TINCR inhibits the proliferation, migration and invasion and promotes the apoptosis of breast cancer cells by suppressing the akt pathway via IGF1R. *Int J Mol Med*. 2020;46(3):989–1002.
31. Cesarini V, Silvestris DA, Tassinari V, Tomaselli S, Alon S, Eisenberg E, et al. ADAR2/miR-589-3p axis controls Glioblastoma cell migration/invasion. *Nucleic Acids Res*. 2018;46(4):2045–59.
32. Murakawa T, Okamoto K, Omiya S, Taneike M, Yamaguchi O, Otsu K. A mammalian mitophagy receptor, Bcl2-L-13, recruits the ULK1 complex to Induce Mitophagy. *Cell Rep*. 2019;26(2):338–e345336.

33. Guo P, Lu J, Lei Y. Significant role of circRNA BBS9 in chronic obstructive pulmonary disease via miRNA-103a-3p/BCL2L13. *BMC Pulm Med.* 2023;23(1):257.
34. Meng F, Zhang L, Zhang M, Ye K, Guo W, Liu Y, et al. Down-regulation of BCL2L13 renders poor prognosis in clear cell and papillary renal cell carcinoma. *Cancer Cell Int.* 2021;21(1):332.
35. Wang J, Chen A, Xue Z, Liu J, He Y, Liu G, et al. BCL2L13 promotes mitophagy through DNM1L-mediated mitochondrial fission in glioblastoma. *Cell Death Dis.* 2023;14(9):585.

### **Publisher's note**

Springer Nature remains neutral with regard to jurisdictional claims in published maps and institutional affiliations.